Acta Technica *62* No. 2B/2017, 231–240

Numerical simulation and experimental study of smelting reduction furnace based on oxygen-rich top-blowing[1]

Yiqin Liu[2,3], Shan Qing[2], Yingchun Liu[2,4], Aimin Zhang[2], Zhao Gui[2]

Abstract. The development and the progress of modern society have made the iron and steel industry facing increasingly severe environmental pressure load and the risk of a shortage of resources. Therefore, it is necessary to develop a new ironmaking technology that can meet the needs of modern economic development and environmental protection. Factor analysis of the numerical simulation of the oxygen-rich top-blowing smelting furnace was carried out by using software of fluid mechanics and related effects. Through the numerical simulation and industrial test monitoring results of comparative analysis, it was found that the results of the two were relatively consistent. This shows that the technology can be applied in specific engineering practice and can promote the healthy development of China's iron and steel industry.

Key words. Oxygen-rich top-blowing, numerical simulation, experiment.

1. Introduction

Since the establishment of Chinese, a thousand things wait to be done. The economy of our country is developing rapidly. In order to meet the production and construction of our country, the output of iron and steel is increasing year by year.

[1]This work reported in National Natural Science Foundation of China: The transfer characteristics and strengthening mechanism of Al2O3/TiO2 nanoparticles in the organic Rankine cycle under multi-field driving, (No. 51566005) and National Natural Science Foundation of China: Phosphorus behavior in smelting reduction process of high phosphorus iron ore in Yunnan based on HIsmelt (No. 51064015).

[2]Department of Metallurgical and Energy Engineering, Kunming University of Science and Technology, Kunming, 650093, China

[3]Department of Communication and Information Engineering, Yunnan Open University, Kunming 650000, China

[4]Corresponding author

China's crude steel production increases from 450 thousand tons in the founding to 100 million tons by 1996. The annual output reached 6.02 tons in 2015 [1]. It is foreseeable that the demand for steel is still great in a long period of time. As long as the supply of coke is enough, the blast furnace ironmaking process is needed to produce and supply the steel. However, the process of blast furnace ironmaking has many deficiencies. On the one hand, the coal resources needed are relatively small. On the other hand, a large amount of air pollution is produced in the process of ironmaking. This is clearly not in line with China's current strategy for the protection of the ecological environment. At the same time, China's coke oven imports from abroad mainly. But the aging of coke ovens in the major steel producing countries around the world makes the supply of coke more stressful, which makes the traditional process of blast furnace facing severe challenges.

Internationally, various countries have begun to carry out extensive research on the new ironmaking process of non-coking coal and iron ore. The utilization of resources is improved and environmental pollution is reduced through new processes. After nearly 30 years of development time, the United States, Japan, Australia and other foreign countries has achieved remarkable results in the new iron making process of the developer, and it has been widely used in actual application promotion. China's iron and steel production has increased year by year, which means that the demand for focusing coal is increasing year by year. The amount of coking coal needed per year must reach 57 thousand and 400 tons [2]. According to the reserves of China's coking coal resources and the demand of our country, it is likely that China will be faced with the depletion of coking coal resources in 2026. Under such circumstances, it is imperative for China to carry out a new type of ironmaking process to reduce or no longer use the coking coal resources.

2. State of the art

Since the latter half of the last century, people have begun to actively attempt to develop and study new types of non-coking coal iron making process. From the initial reduction process to the current smelting reduction process, many countries in the world have invested a lot of material and financial resources, and made outstanding achievements in South Korea. Among them, there are typical Jindal steel mills in India, Saldanha in South Africa and POXCO. They have built many large demonstration plants by using the new smelting reduction process, and actively seek investment in order to achieve commercial production [3]. The most important feature of the new iron making process is the direct use of iron ore and coal that have not been treated. It uses direct reduction process to directly iron ore into solid iron, or it uses the smelting reduction process to realize the reduction reaction of iron ore in the high temperature slag phase [4].

Through the existing research and new technology, it can be seen that the new iron smelting process can skip the sintering of iron ore and the process of coking coal compared to the traditional iron smelting process. In this way, the economic benefits of ironmaking can be improved while the pollution to the environment is reduced. The comparison and analysis of all kinds of new iron making process shows

that smelting reduction method has very good potential and research value. It can make use of the high temperature environment provided by the combustion of coal so that the molten iron can be melted and reduced to be molten iron. The reaction rate is faster. The strength of molten iron smelting by this method is more than 5 times of that of blast furnace [5].

3. Methodology

3.1. Mathematical model for oxygen-rich top-blowing smelting reduction furnace

The flow of fluid is satisfied with the conservation equations of physics, which includes the conservation of energy, the conservation of mass, and the conservation of momentum (Weiland et al. 2013 [8]). If the flow of fluids has different components and can be burned with each other, additional component transport equations are needed. If the studied fluid is turbulent, the turbulent transport equation needs to be further considered [6]. We need to consider the turbulent combustion reaction to construct the mathematical model, and the basic equations are as follows:

The continuity equation of mass conservation equation is

$$\frac{\partial(\rho)}{\partial t} + \operatorname{div}\ (\rho U)\ , \tag{1}$$

where ρ is the fluid density, U is the free velocity and t is the time.

The momentum conservation component equations may be written in the form

$$\frac{\partial(\rho u)}{\partial t} + \operatorname{div}\ (\rho u U) = \operatorname{div}\ (\mu \operatorname{grad}\ u) - \frac{\partial p}{\partial x} + S_u\,, \tag{2}$$

$$\frac{\partial(\rho v)}{\partial t} + \operatorname{div}\ (\rho v U) = \operatorname{div}\ (\mu \operatorname{grad}\ v) - \frac{\partial p}{\partial x} + S_v\,, \tag{3}$$

$$\frac{\partial(\rho w)}{\partial t} + \operatorname{div}\ (\rho w U) = \operatorname{div}\ (\mu \operatorname{grad}\ w) - \frac{\partial p}{\partial x} S_w\,, \tag{4}$$

where u, v, w are the components of velocity in three dimensions and p is the internal stress tensor of fluid.

The energy conversation equation is

$$\frac{\partial(\rho T)}{\partial t} + \operatorname{div}\ (\rho T U) = \operatorname{div}\ \left(\frac{\lambda}{C_{\mathrm{r}}} \operatorname{grad}\ T\right) + S_r\,. \tag{5}$$

Here, T is the fluid temperature, λ is the fluid volume viscosity and C is an empirical coefficient.

By arranging the equations in front, the following general equation can be obtained

$$\frac{\partial(\rho\phi)}{\partial t} + \operatorname{div}\ (\rho\phi U) = \operatorname{div}\ (\Gamma_\phi \operatorname{grad}\ \phi) + S_\phi\,. \tag{6}$$

In the preceding equation, ϕ represents a generic variable that can be used to represent variables such as u, v, w and T in the governing equations. Symbols S_ϕ and Γ_ϕ represent diffusion and generalized source terms [7]. In formula (6), the items from left to right are represented as transient terms and convection terms, respectively. And from left to right, they are diffusion terms and source terms, respectively.

3.2. Establishment of geometric model of smelting reduction furnace

The main research model is used in cylindrical geometry of the model is relatively simple, less difficult when rendering 3D geometry of the GAMBIT can be used to draw three-dimensional graphics rendering of the smelting reduction furnace, as shown in Fig. 1. The calculation area is mainly composed of a smelting reduction furnace, in addition to a combustion nozzle and a part of the flue area. In the process of simulation, it is unnecessary to carry out the calculation of the combustion nozzle, so the modeling of the spray gun is not necessary when the geometric model is built, but only the exit section of the nozzle jet flow is taken into account. After the completion of the collection model, it is necessary to partition the grid, and the quality of grid partition will have a very important impact on the accuracy of the entire process and the accuracy and economy of the results.

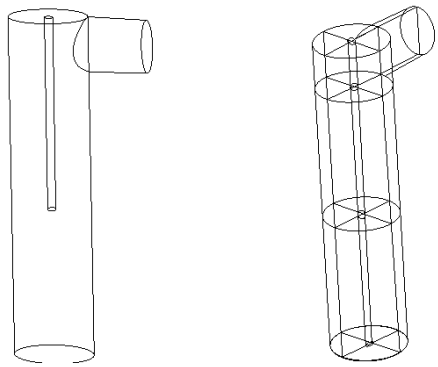

Fig. 1. The model for the reduction of oxygen top blown melting furnace

In order to obtain excellent mesh quality, (Milbourne et al. 2013) [9], it can be divided into different regions. According to this method, the main part of the smelting reduction furnace can be divided into 3 zones, and the results are shown in Fig. 2 (furnace mesh and flue grid, respectively). In order to improve the mesh quality as much as possible, the cylinder is divided into 4 equal volume fan-shaped columns along the axial direction. Each column is 90 degrees in the ground, and is divided into hexahedral regular network. But the flue and the cylinder intersecting part to be divided into hexahedron regular mesh is difficult, and divide it into tetrahedral meshes according to the situation, because this part is only in the whole grid occupies a small proportion, this also shows that the quality of the entire grid. When the

central cylinder is meshed, it is necessary to take into account the characteristics of the jet region in the central cylinder region, and its gradient is relatively large, so it is necessary to encrypt the mesh.

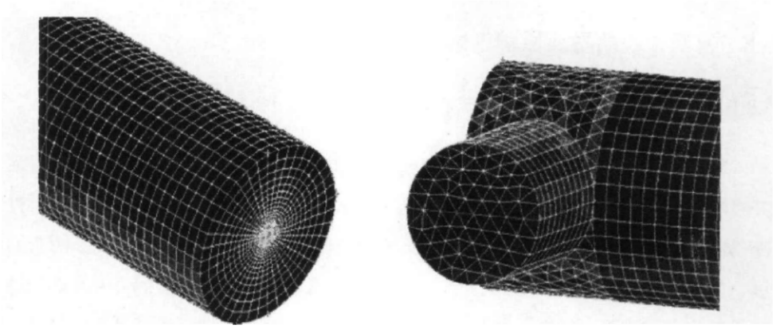

Fig. 2. Mesh diagram of oxygen top blown smelting reduction furnace

In the simulation of the model, the fuel oil is injected from the source into the furnace with the form of discrete phase, in which the air is joined by continuous phase [10]. The burner is not involved in the calculation, which simplifies the calculation. The fuel injector and the air inlet can be simplified into two surfaces [11]. The fuel oil can be selected according to the actual needs of the appropriate atomization model, and will not be affected by the model inlet conditions.

By studying the combustion temperature distribution of different fuels, the temperature field distribution under 21 %, 35 % and 46 % oxygen-enriched concentration was analyzed respectively [12]. The analysis results show that the average temperature of fuel combustion increases with the increase of oxygen enrichment concentration, and the combustion state tends to be stable. This is mainly because the effect of volume of combustion products on combustion temperature is remarkable. If oxygen or air is replaced by oxygen enriched air or nitrogen as an oxidant in combustion reactions, the volume of combustion products will be reduced significantly. The combustion temperature increases with the increase of oxygen concentration, and the distance of ignition is shortened, and the high temperature zone at the bottom of the furnace is further expanded [4]. However, because of more than 70 % heat and mass transfer in the furnace are realized based on the radiation, the increase of the oxygen content is accompanied by a decrease in radiation gases such as carbon dioxide, which is not conducive to the temperature in the furnace to improve the heat transfer and radiation. It is also true that when the oxygen enrichment concentration in the furnace is greater than 50 %, the effect of oxygen concentration on the temperature rise is not obvious.

In the numerical simulation, the exit cross section of the model is monitored. The parameters of different combustion furnace outlet oxygen concentration under top-blowing smelting reduction furnace, and the specific test results are shown in Table 1 [2]. As a result of the monitoring of the export section, the total amount of oxygen, nitrogen, water, and nitric oxide and nitrogen dioxide is about 100 %. In addition, carbon smoke is not monitored. The amount of carbon monoxide in the

monitoring results is relatively small, indicating that the furnace then reacts fully. The oxygen content is too large, and it shows that the combustion in the furnace is an excessive combustion of air, which is conducive to the full and complete combustion of combustion [13].

Table 1. Exit parameter

Oxygen density (%)	Average temperature (K)	Mass fraction of each component (%)					Exit velocity (m/s)
		O_2	CO	N_2	H_2O	CO_2	
21	1715.2	4.32	0.64	78	3.74	12.30	4.56
35	1853.3	4.12	0.57	66	7.47	22.84	4.04
46	1920.5	9.98	0.52	53	9.96	31.56	3.68

3.3. Raw materials and test scheme in the oxygen top-blowing smelting reduction experiment

According to the previous design ideas, the oxygen top-blowing smelting reduction experiment was studied. The raw materials used included anthracite and high phosphorus iron ore. They were mixed with MgO, fluorite and lime in a certain proportion, and then added to the furnace after mixing. The design idea of the test scheme is as follows:

The smelting reduction of high phosphorus iron ore was carried out by using P = 0.9 % alone, so as to obtain the best control parameter for smelting high phosphorus iron ore. The smelting reduction of high phosphorus iron ore was carried out using root mineral (P = 0.305 %) alone. The industrial test of amalgamation and reduction of Huimin mine and root ore according to the ratio of P = 0.7 % and P = 0.5 % was carried out. In the reduction reaction, high phosphorus iron ore and bituminous coal with C/O = 1.1 and R = 2.0 were added. In order to improve the fluidity of slag iron and be easy to separate, 1% CaF_2 of slag and 4% MgO were added.

Table 2. Test parameters

Oxygen density (%)	Oxygen flow rate (m^3/h)	Thermocouple temperature (°C)	Smoke analyzer reading							
			O_2 (%)	CO (mg/m^3)	NO (mg/m^3)	NO_2 (mg/m^3)	SO_2 (mg/m^3)	CO_2 (%)	Speed (m/s)	Temperature (°C)
21–30	30–37	1350–1410	2.31	327	623	731	156	14.65	4.33	1029
31–40	27–33	1450–1530	4.01	436	568	607	190	25.24	3.78	1137
41–50	23–30	1495–1580	3.14	355	495	533	186	33.52	3.46	1190
51–60	21–27	1500–1590	2.55	334	467	512	167	33.46	3.19	1216
61–70	20–25	1480–1590	2.71	319	451	598	182	34.25	2.89	1215

After the prepared reduced molten iron was cooled, it was put into the crucible for grinding and the sample of 500 g was obtained. The sample was placed in a high temperature furnace and was continuously heated up to 1450°C. At this temperature level, it was cooled down gradually after holding the temperature for 1.5 h. When the temperature was reduced to normal temperature, samples were taken and analyzed accordingly. The chemical analysis, SRD analysis and SEM analysis at different stages of molten iron and slag prepared by the oxygen-rich top-blowing smelting reduction ironmaking furnace were carried out. During each experiment, measurement and analysis were needed to determine the effect of smelting under different experiment parameters.

4. Result analysis and discussion

4.1. Comparison of the results of oxygen-rich top-blowing smelting reduction experiments and numerical simulation results

The chemical analysis of oxygen-rich top-blowing smelting reduction experiments under different conditions of molten iron and slag is shown in Table 3.

Table 2. Test parameters

Fused reduced iron							Temperature	Smelting reduction slag			
T.F	M.F	S	P	C	Si	M	°C	MgO	CaO	SiO_2	Al_2O_3
98.01	95.36	0.16	0.15	0.95	0.37	75.68	1526	13.26	47.19	8.23	15.32

The sample obtained was subjected to X-ray diffraction analysis to observe the presence of reduced iron. As a result, the comparison results of the standard diffraction pattern of metal iron X-ray diffraction and ray diffraction were obtained, as shown in Fig. 4. It could be seen from the figure that in the X-ray diffraction patterns of smelting reduction iron, the most important was the line of iron, and the iron was in the form of iron, as well as part of the Fe_2O_3, FeO and Fe_3O_4. In addition, the spectra of some small amounts of C were also included in the spectra, which was due to the excess pulverized coal. In addition to heating and reducing agent consumption, this part of coal powder also had C penetration in some pulverized coal.

4.2. Comparison of smoke monitoring at outlet

Through simulation and experimental monitoring of temperature, the analysis and comparison was carried out. The numerical simulation results showed that when the oxygen concentration was 21 %, 35 % and 46 %, the corresponding 2100 K, 2250 K and 2280 K were converted, and the actual combustion temperature was 1386 °C, 1504.5 °C and 1528.3 °C, respectively. Based on the comparative analysis

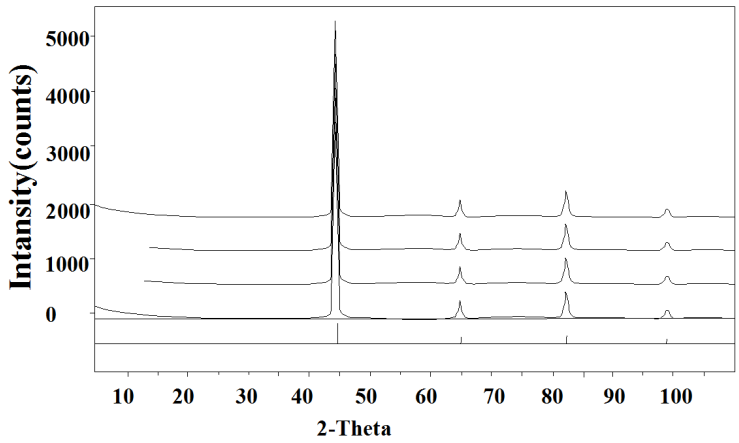

Fig. 3. XRD diagram of fused reduced iron

of the results of the oxygen-rich top-blowing smelting reduction experiments, it was found that the oxygen concentration of 21 %∼30,% corresponded to the temperature of 1350 °C to 1410 °C. When the concentration of oxygen was between 31 % and 40 %, the corresponding temperature was between 1450 °C and 1530 °C. When the concentration of oxygen was between 41 % and 50 %, the corresponding temperature was between 1495 °C and 1580 °C. After the numerical simulation, the converted temperature is 1386 °C, 1504.5 °C and 1528.2 °C, respectively, and the temperature was fluctuated in the range of the experimental data. This showed that the measured results of thermocouples were in good agreement with the numerical simulation results.

Numerical calculation and experimental monitoring results were compared and analyzed. By simulation, it could be seen that when the oxygen concentration was 21 %, 35 % and 46 %, the average temperature of flue gas outlet is 1081.6 °C, 1176.7 °C and 1239.5 °C, respectively. The temperature under the different oxygen concentration measured by the smoke analyzer in the test was shown as follows. When the oxygen concentration was 21 %∼30 %, 31 %∼40 %, and 41 %∼50 %, the corresponding flue gas temperature was 1029 °C, 1136 °C, and 1198 °C, respectively. By comparing and analyzing, it could be seen that the results measured by the experiments and the results of numerical simulation were close. However, the temperature of flue gas analyzer was slightly lower because of the loss of energy in the process of the experiments.

A comparative analysis of smoke flow velocity was carried out by monitoring and numerical simulation. In the numerical simulation, when the oxygen concentration was 21 %, 35 % and 46 %, the average velocity of flue gas at the corresponding outlet was 4.57 m/s, 4.03 m/s, 3.68 m/s, respectively. Correspondingly, when oxygen concentrations were 21 %∼30 %, 31 %∼40 %, and 41 %∼50 %, the average speed of smoke monitoring at the exit was 4.32 m/s, 3.97 m/s, 3.41 m/s, respectively. By comparing and analyzing, it could be seen that the results measured by the exper-

iment was similar to the results of numerical simulation analysis. However, due to the possibility of collisions between the fly ash and flue gas in the process of flue gas flow, partial energy loss occurred, which led to a decrease in velocity.

Through monitoring and numerical simulation of oxygen content in flue gas outlet, we could see that in the numerical simulation, when the oxygen concentration was 21 %, 35 % and 46 %, the corresponding oxygen content in the flue gas at the outlet was 4.31 %, 4.13 %, 3.97 %, respectively. When the concentration of oxygen in the flue gas at the exit was 21 %∼ 30%, 31 %∼ 40%, and 41 %∼50 %, the oxygen content in the flue gas at the corresponding outlet was 2.31 %, 4.01 %, 3.14 %, respectively. The comparison found that the two of them were identical, and no oxygen was found.

5. Conclusion

Under the new social situation, the traditional iron and steel production process is difficult to meet the needs of economic efficiency and environmental protection. Therefore, more economical and environmentally friendly production processes need to be replaced. In this paper, the mathematical model of oxygen-rich top-blowing smelting reduction furnace was constructed by software. Firstly, the study on air coefficient, furnace temperature and oxygen enriched combustion was carried out, so as to construct the mathematical model. The influence factors of oxygen jet, combustion, combustion temperature distribution and combustion characteristics were analyzed. By comparing and analyzing the monitoring results and the results of numerical simulation in the furnace, the deviation of the results of industrial test and numerical simulation were obtained. The results show that under different oxygen concentrations, the temperature of the furnace, the average temperature of the flue gas outlet, the velocity of the smoke flow and the oxygen content of the smoke outlet are in good agreement with the monitoring results. However, it is necessary to further improve the applicability and reliability of the model, so as to achieve better application results in engineering practice.

References

[1] S. J. Mangena, J. R. Bunt, F. B. Waanders: *Mineralogical behaviour of North Dakota lignite in an oxygen/steam blown moving bed reactor*. Fuel Processing Technology *106* (2013), 474–482.

[2] J. H. Wei, T. Li: *Study on mathematical modeling of combined top and bottom blowing VOD refining process of stainless steel*. Steel Research International *86* (2015), No. 3, 198–211.

[3] J. Krzywanski, W. Nowak: *Artificial intelligence treatment of SO_2 emissions from CFBC in air and oxygen-enriched conditions*. Journal of Energy Engineering *142* (2016), No. 1, paper 04015017.

[4] A. C. Gujar, J. Baik, N. Garceau, N. Muradov, A. T-Raissi: *Oxygen-blown gasification of pine charcoal in a top-lit downdraft moving-hearth gasifier*. Fuel *118* (2014), 27–32.

[5] Y. D. Kim, C. W. Yang, B. J. Kim, K. S. Kim, J. W. Lee, J. H. Moon, W. Yang,

T. U. Yu, U. D. Lee: *Air-blown gasification of woody biomass in a bubbling fluidized bed gasifier.* Applied Energy *112* (2013), 414–420.

[6] J. H. Kim, S. Schouten, M. Rodrigo-Gámiz, S. Rampen, G. Marino, C. Huguet, P. Helmke, R. Buscail, E. C. Hopmans, J. Pross, F. Sangiorgi, J. B. M. Middelburg, J. S. Sinninghe Damsté: *Influence of deep-water derived isoprenoid tetraether lipids on the $TEX_8$6 H paleothermometer in the Mediterranean Sea.* Geochimica et Cosmochimica Acta *150* (2015), 125–141.

[7] Z. Y. Wang, J. L. Zhang, X. D. Xing, Z. J. Liu: *Congregated electron phase and Wagner model applied in titanium distribution behavior in low-titanium slag.* Transactions of Nonferrous Metals Society of China *25* (2015), No. 5, 1640–1647.

[8] F. Weiland, H. Hedman, M. Marklund, H. Wiinikka, O. Öhrman, R. Gebart: *Pressurized oxygen blown entrained-flow gasification of wood powder.* Energy & Fuels *27* (2013), No. 2, 932–941.

[9] R. J. Milbourne, T. R. Meadowcroft: *The use of an oxygen-blown open hearth to feed a multistrand casting machine.* Canadian Metallurgical Quarterly *7* (1968), No. 4, 247–253.

[10] M. Naqvi, J. Yan E. Dahlquist: *System analysis of dry black liquor gasification based synthetic gas production comparing oxygen and air blown gasification systems.* Applied Energy *112* (2013), 1275–1282.

[11] E. Simeone, M. Siedlecki, M. Nacken, S. Heidenreich, W. de Jong: *High temperature gas filtration with ceramic candles and ashes characterisation during steam–oxygen blown gasification of biomass.* Fuel *108* (2013), 99–111.

[12] G. Zhang, Y. Yang, H. Jin, G. Xu, K. Zhang: *Proposed combined-cycle power system based on oxygen-blown coal partial gasification.* Applied Energy *102* (2013), 735 to 745.

[13] P. Jin, Z. Jiang, C. Bao, Y. Lu, J. Zhang, X. Zhang: *Mathematical modeling of the energy consumption and carbon emission for the oxygen blast furnace with top gas recycling.* Steel Research International *87* (2013), No. 3, 320–329.

Received May 7, 2017